

Simulation Model for the Solution Copolymerization of Acrylonitrile and Styrene in Azeotropic Composition

CHEN-CHONG LIN, WEN-YEN CHIU, and CHIOU TONG WANG,
National Taiwan University, Taipei, Taiwan, China

Synopsis

The rate of chemical-initiated solution copolymerization of acrylonitrile and styrene in toluene as solvent was studied theoretically and experimentally with a limiting conversion of about 50%. Taking into consideration industrial operation, the polymerization was carried out under an azeotropic composition of AN:St = 25:75 by weight, and a new kinetic model is proposed for estimating the conversion and the rate of polymerization as well as the molecular weight distribution over the entire reaction course. It is shown that the experimental data of conversion and the rate of reaction, as well as average molecular weight, can be successfully correlated to limiting conversion by this model if the effect of change in the initiator efficiency during the reaction on the rate of reaction is taken into consideration. It was found that the effective initiator efficiency can be expressed as $f = 0.0956([A_0] + [S_0])$. Some important kinetic constants as well as model parameters are obtained by simulation of this model, which agree with the experimental results. Certain transfer constants obtained by this simulation model are $k_{f12} = 30 \times k_{f11}$ and $k_{f21} = 5 \times k_{f22}$. Within the limiting conversion studied, no significant autoacceleration is observed. It is therefore not necessary to include this effect in the model.

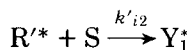
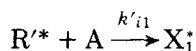
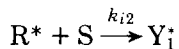
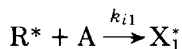
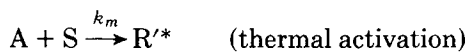
INTRODUCTION

Acrylonitrile-styrene copolymers are thermoplastic polymers of increasing commercial importance. Among the polymerization operations, the solution process is often the method of choice because of low viscosity of the system. The advent of the vented extruder helped greatly in this process, providing an effective means to degas or devolatilize the highly volatile materials. Along with the development of the techniques of the polymerization process, many advances are necessary in the understanding of the actual mechanism of the reaction and what one must do in the polymerization in reference to time, temperature, and other variables to make the most acceptable products with good performance. In industry, it is especially important to include the rate of polymerization and the size distribution of the polymer formed simultaneously as a function of the operation variables. Many previous works have tried to deal with the modeling of polymerization reactors.¹⁻⁴ But quite few have succeeded in solving the resulting differential rate equations to predict the conversion as well as the molecular weight distribution as a function of time due to the extreme difficulty of obtaining a suitable simulation model and, in turn, the rate constants as well as model parameters.⁵⁻⁷ The present work proposes a kinetic model for the solution copolymerization of acrylonitrile and styrene in toluene as solvent under the industrially important azeotropic composition of monomers which can simulate conversion data and molecular weight distribution features for the design of practical reactors.

SIMULATION MODEL OF REACTION KINETICS

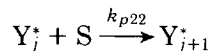
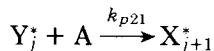
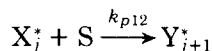
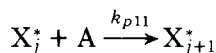
The following is the kinetic model of a chemical-initiated free-radical copolymerization in solution.

Initiation:

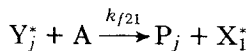
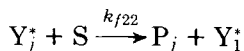
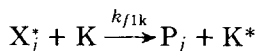
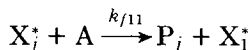
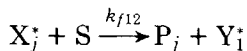


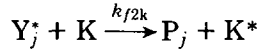
Because $k_{p12} = k_{p11}/0.06$ and $k_{p21} = k_{p22}/0.386$ as listed in Table II,⁸ thermal initiations of $A + A$ and $S + S$ are minor comparing with that of $A + S$, and thus they are negligible by kinetic analysis of this model.

Propagation:

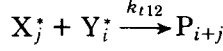
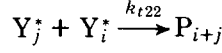
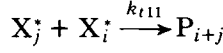


Chain Transfer:





Termination (only the recombination is considered):



On the basis of the foregoing set of reactions, the following equations can be derived:

$$[I] = [I_0] \exp(-k_d t) \tag{1}$$

$$R_i = 2f k_d [I] + k_m \eta [A]^a [S]^b \tag{2}$$

where η is a correction factor being due to the thermal initiations of A + A and S + S, and a and b are constants:

$$\frac{-d[A]}{dt} \simeq k_{p11}[A]X_T + k_{p21}[A]Y_T \tag{3}$$

$$\frac{-d[S]}{dt} \simeq k_{p12}[S]X_T + k_{p22}[S]Y_T \tag{4}$$

$$\frac{-d([A] + [S])}{dt} \simeq k_{p11}[A]X_T + k_{p21}[A]Y_T + k_{p12}[S]X_T + k_{p22}[S]Y_T \tag{5}$$

where

$$X_T = \sum_{j=1}^{\infty} [X_j^*], \quad Y_T = \sum_{j=1}^{\infty} [Y_j^*]$$

$$R_t = 2k_{t12}X_T Y_T + k_{t11}X_T^2 + k_{t22}Y_T^2 \tag{6}$$

Under the steady-state assumption, the following equations will be valid:

$$\frac{dX_T}{dt} = k_{p21}[A]Y_T - k_{p12}[S]X_T = 0 \tag{7}$$

$$\frac{dY_T}{dt} = k_{p12}[S]X_T - k_{p21}[A]Y_T = 0 \tag{8}$$

$$Y_T = \frac{k_{p12}[S]}{k_{p21}[A]} X_T \tag{9}$$

In the other hand,

$$R_i = R_t \tag{10}$$

where ϕ will not change significantly until 50% conversion, and substituting eq. (9) into eq. (6) and letting

$$\phi = 2k_{t12} \frac{k_{p12}[S]}{k_{p21}[A]} + k_{t11} + k_{t22} \left(\frac{k_{p12}[S]}{k_{p21}[A]} \right)^2 \tag{11}$$

then the following relations can be obtained:

$$R_i = X_T^2 \phi \tag{12}$$

$$X_T = (R_i/\phi)^{1/2} \quad (13)$$

$$Y_T = \frac{k_{p12}[S]}{k_{p21}[A]} (R_i/\phi)^{1/2} \quad (14)$$

Finally, the rate of solution copolymerization, R_p , can be represented by

$$R_p = \frac{-d([A] + [S])}{dt} = k_{p11}[A] \left(\frac{R_i}{\phi}\right)^{1/2} + 2k_{p12}[S] \left(\frac{R_i}{\phi}\right)^{1/2} + k_{p22}[S]^2 \frac{k_{p12}}{k_{p21}[A]} \left(\frac{R_i}{\phi}\right)^{1/2} \quad (15)$$

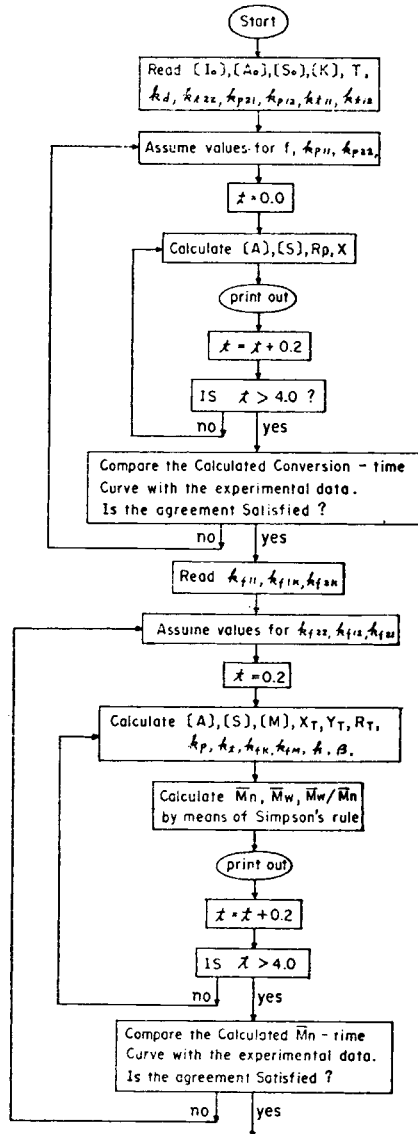


Fig. 1. Flow chart of computer program for the simulation model.

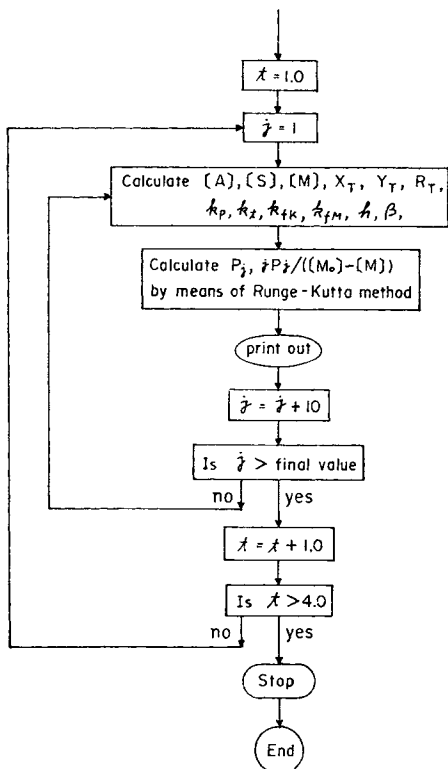


Fig. 1 (Continued from previous page.)

In order to produce a commercially applicable composition, an azeotropic composition of monomers is maintained to prevent a composition shift during the polymerization course. It is known that the azeotropic composition of acrylonitrile-styrene is 25:75 by weight, or 1:1.53 by mole. Accordingly,

$$[S]/[A] = 1.53 \tag{16}$$

and R_p can be represented by

$$R_p = -2.53 \frac{d[A]}{dt} = k_{p11}[A] \left(\frac{R_i}{\phi}\right)^{1/2} + (2 \times 1.53)k_{p12}[A] \left(\frac{R_i}{\phi}\right)^{1/2} + (1.53)^2[A] \frac{k_{p12}k_{p22}}{k_{p21}} \left(\frac{R_i}{\phi}\right)^{1/2} \tag{17}$$

The parameter ϕ as defined in eq. (11) is found experimentally to be merely a constant in this solution copolymerization system. Namely,

$$\phi = (2 \times 1.53) \frac{k_{t12}k_{p12}}{k_{p21}} + k_{t11} + (1.53)^2k_{t22} \left(\frac{k_{p12}}{k_{p21}}\right)^2 \tag{18}$$

The conversion is also simplified as

$$X = \frac{53[A_0] + 104[S_0] - (53[A] + 104[S])}{53[A_0] + 104[S_0]} = \frac{[A_0] - [A]}{[A_0]} \tag{19}$$

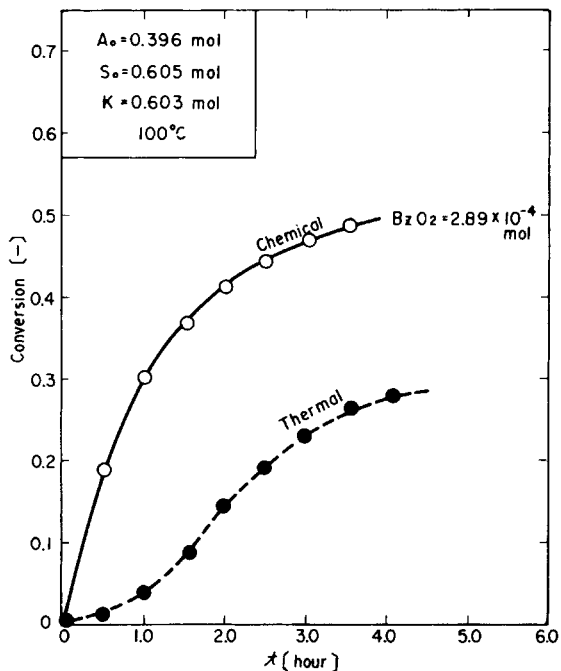


Fig. 2. Experimental conversion vs. time with and without initiator: (—) $\text{BzO}_2 = 2.89 \times 10^{-4}$ mole; (---) $\text{BzO}_2 = \text{none}$; $A_0 = 0.396$ mole; $S_0 = 0.605$ mole; $K = 0.603$ mole; 100°C .

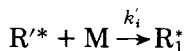
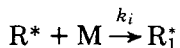
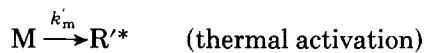
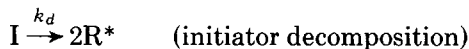
An unit segment of the copolymer represented by M can be defined as 1.53/2.53 molecules with styrene and 1/2.53 molecules with acrylonitrile, where it has a molecular weight of $104 \times (1.53/2.53) + 53 \times (1/2.53)$ as a unit segment. So it is defined as

$$[\text{M}] = [\text{A}] + [\text{S}] \quad (20)$$

$$R_T = X_T + Y_T \quad (21)$$

The process of an azeotropic copolymerization is now simplified to the following homopolymerization scheme:

Initiation:



Instead of eq. (2), we rewrite the initiation step as

$$R_i = 2fk_d[\text{I}] + k'_m \eta' [\text{M}]^m \quad (22)$$

$$k'_m \eta' = \frac{k_m \eta [\text{A}]^a [\text{S}]^b}{([\text{A}] + [\text{S}])^m} \quad (23)$$

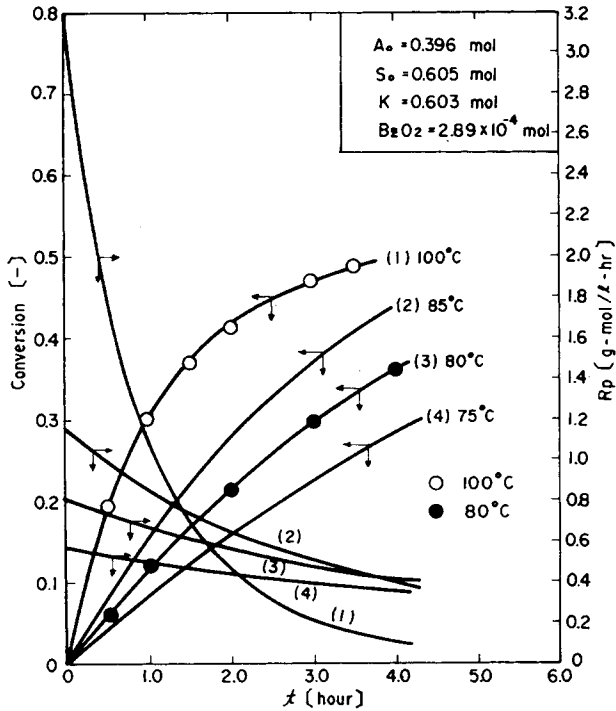
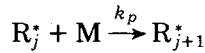


Fig. 3. Effect of reaction temperature and rate of polymerization as function of time. (Two sets of experimental data are represented by points.)

Propagation:



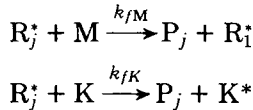
Instead of eq. (5), we rewrite the propagation step as

$$\begin{aligned} \frac{-d[M]}{dt} &\simeq k_p[M]R_T = k_p([A] + [S])(X_T + Y_T) \\ &= k_{p11}[A]X_T + k_{p21}[A]Y_T + k_{p12}[S]X_T + k_{p22}[S]Y_T \end{aligned} \quad (24)$$

and

$$k_p = \frac{k_{p11}[A]X_T + k_{p21}[A]Y_T + k_{p12}[S]X_T + k_{p22}[S]Y_T}{([A] + [S])(X_T + Y_T)} \quad (25)$$

Chain Transfer:



$$\begin{aligned} k_{fM}R_T[M] &= k_{fM}(X_T + Y_T)([A] + [S]) \\ &= k_{f12}X_T[S] + k_{f11}X_T[A] + k_{f22}Y_T[S] + k_{f21}Y_T[A] \end{aligned} \quad (26)$$

and

$$k_{fM} = \frac{k_{f12}X_T[S] + k_{f11}X_T[A] + k_{f22}Y_T[S] + k_{f21}Y_T[A]}{(X_T + Y_T)([A] + [S])} \quad (27)$$

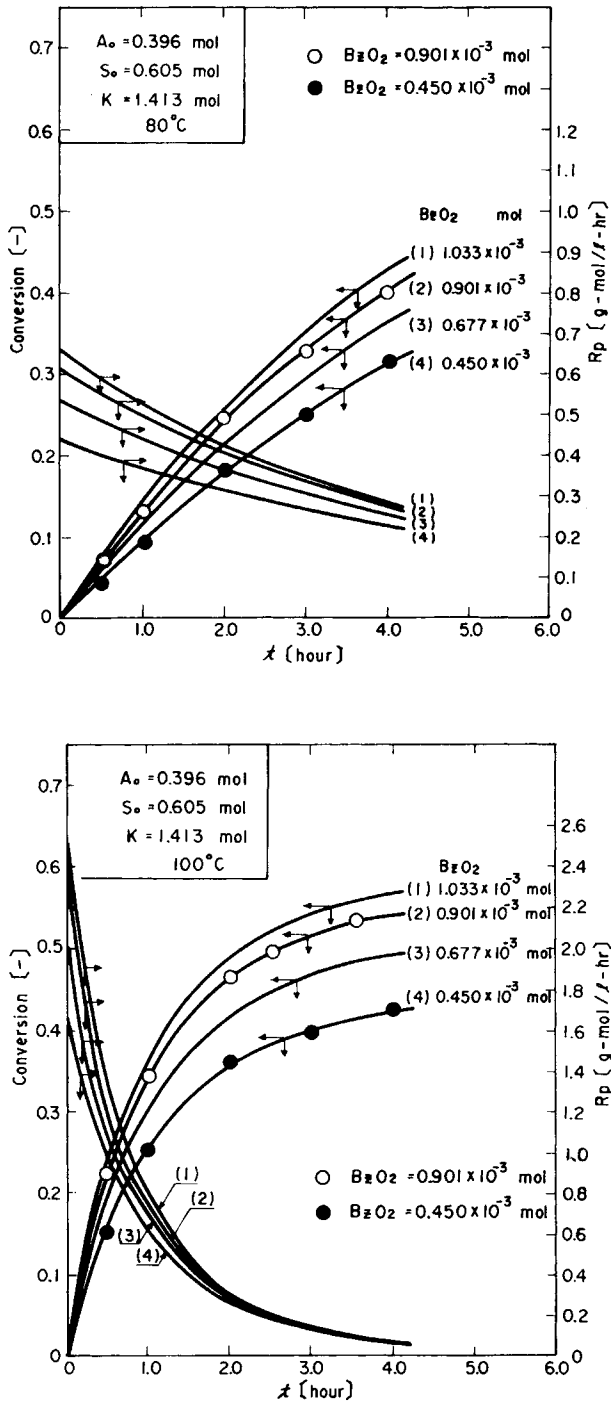


Fig. 4. Effect of initiator concentration on conversion and rate of polymerization as function of time under reaction temperature of 80°C (a) and 100°C (b). (Two sets of experimental data are represented by points.)

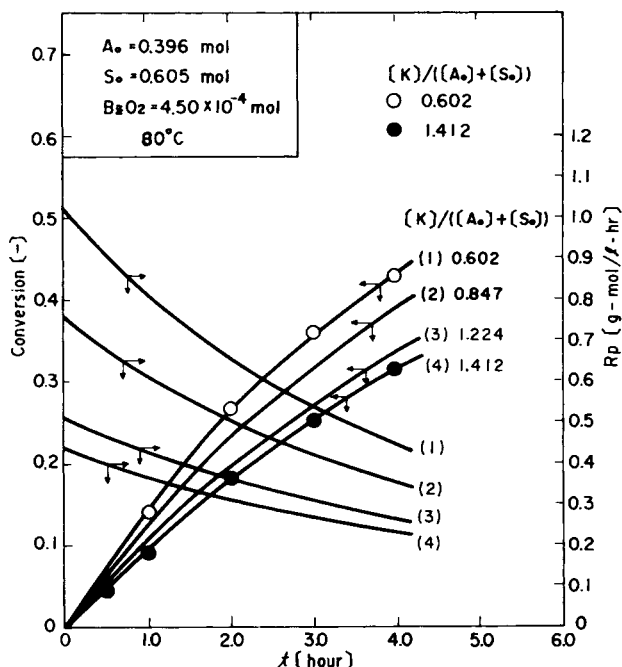


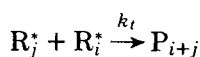
Fig. 5. Effect of solvent-monomer ratio on conversion and rate of polymerization as function of time under reaction temperature of 80°C (a) and 100°C (b). (Two sets of experimental data are represented by points.)

$$k_{fK}R_T[K] = k_{f1K}X_T[K] + k_{f2K}Y_T[K] \quad (28)$$

and

$$k_{fK} = \frac{k_{f1K}X_T + k_{f2K}Y_T}{(X_T + Y_T)} \quad (29)$$

Termination:



Instead of eq. (6), we rewrite the termination step as

$$R_t = k_t R_T^2 = k_t (X_T + Y_T)^2 = 2k_{t12}X_T Y_T + k_{t11} X_T^2 + k_{t22} Y_T^2 \quad (30)$$

and

$$k_t = \frac{2k_{t12}X_T Y_T + k_{t11} X_T^2 + k_{t22} Y_T^2}{(X_T + Y_T)^2} \quad (31)$$

The polymerization constants for k'_m , k_p , k_{fM} , k_{fK} , and k_t can be obtained from eqs. (23), (25), (27), (29), and (31), respectively, by computer simulation.

Again, according to the steady-state assumption for all the radicals,

$$\frac{d([R^*] + [R'^*])}{dt} = R_i - k_i[R^*][M] - k'_i[R'^*][M] = 0 \quad (32)$$

$$R_i = k_i[R^*][M] + k'_i[R'^*][M] \quad (33)$$

Let

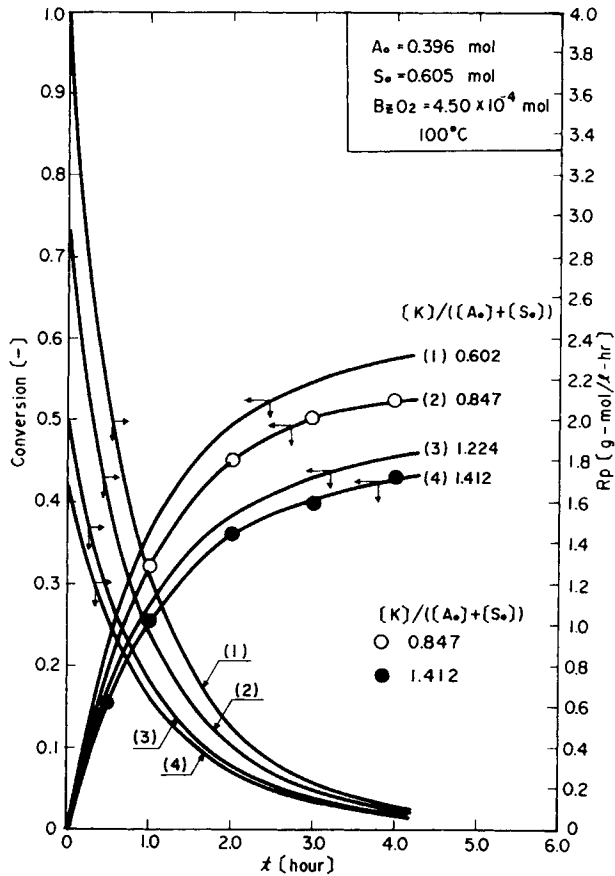


Fig. 5. (Continued from previous page.)

$$\frac{d[R_1^*]}{dt} = 0 \quad (34)$$

It yields for $[R_1^*]$

$$[R_1^*] = h\beta \quad (35)$$

where

$$h = \frac{R_i + (k_{fK}[K] + k_{fM}[M])R_T}{k_p[M]} \quad (36)$$

$$\beta = \frac{k_p[M]}{k_p[M] + (k_{fK}[K] + k_{fM}[M]) + k_t R_T} \quad (37)$$

To use eqs. (36) and (37), it is necessary to insert the proper values for k_{fK} and k_{fM} of the system being studied.

Again let

$$\frac{d[R_j^*]}{dt} = 0 \quad (38)$$

Similarly, it yields for $[R_j^*]$

$$[R_j^*] = \beta[R_{j-1}^*] \quad (39)$$

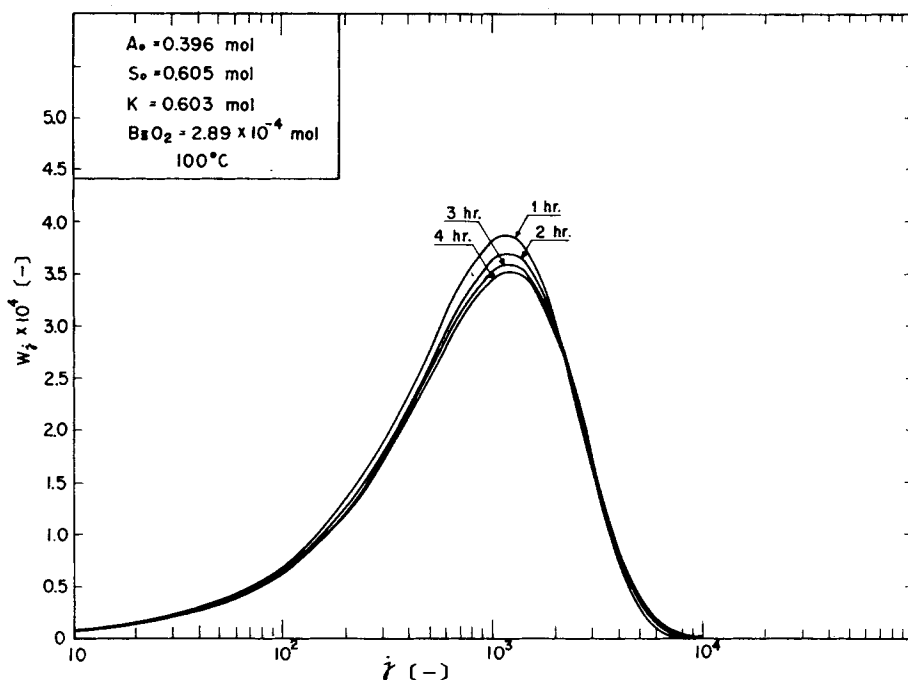


Fig. 6. Molecular weight distribution of copolymer obtained by computer simulation.

By expanding eq. (39), the living radical concentrations with different chain lengths can be shown as

$$\begin{aligned}
 [R_1^*] &= h\beta \\
 [R_2^*] &= \beta[R_1^*] = h\beta^2 \\
 [R_3^*] &= \beta[R_2^*] = h\beta^3 \\
 &\vdots \quad \quad \quad \vdots \\
 [R_j^*] &= \beta[R_{j-1}^*] = h\beta^j
 \end{aligned} \tag{40}$$

If the termination occurs mostly by recombination, the formation of dead polymer with a certain chain length is

$$\begin{aligned}
 \frac{d[P_j]}{dt} &= (k_{fK}[K] + k_{fM}[M])[R_j^*] + \frac{1}{2}k_t \sum_{n=1}^{j-1} [R_n^*][R_{j-n}^*] \\
 &= (k_{fK}[K] + k_{fM}[M])h\beta^j + \frac{1}{2}k_t h^2 \sum_{n=1}^{j-1} \beta^n \beta^{j-n} \\
 &= (k_{fK}[K] + k_{fM}[M])h\beta^j + \frac{1}{2}k_t h^2 (j-1)\beta^j
 \end{aligned} \tag{41}$$

For weight fraction of polymer P_j in total polymer, it gives

$$W_j = j[P_j] / \sum_{j=1}^{\infty} j[P_j] = j[P_j] / ([M_0] - [M]) \tag{42}$$

For number-average chain length, it gives

$$\bar{P}_n = \frac{\sum_{j=1}^{\infty} j[P_j]}{\sum_{j=1}^{\infty} [P_j]} = \frac{[M_0] - [M]}{\sum_{j=1}^{\infty} \int_0^t (d[P_j]/dt) dt} = \frac{[M_0] - [M]}{\int_0^t \sum_{j=1}^{\infty} (d[P_j]/dt) dt} \tag{43}$$

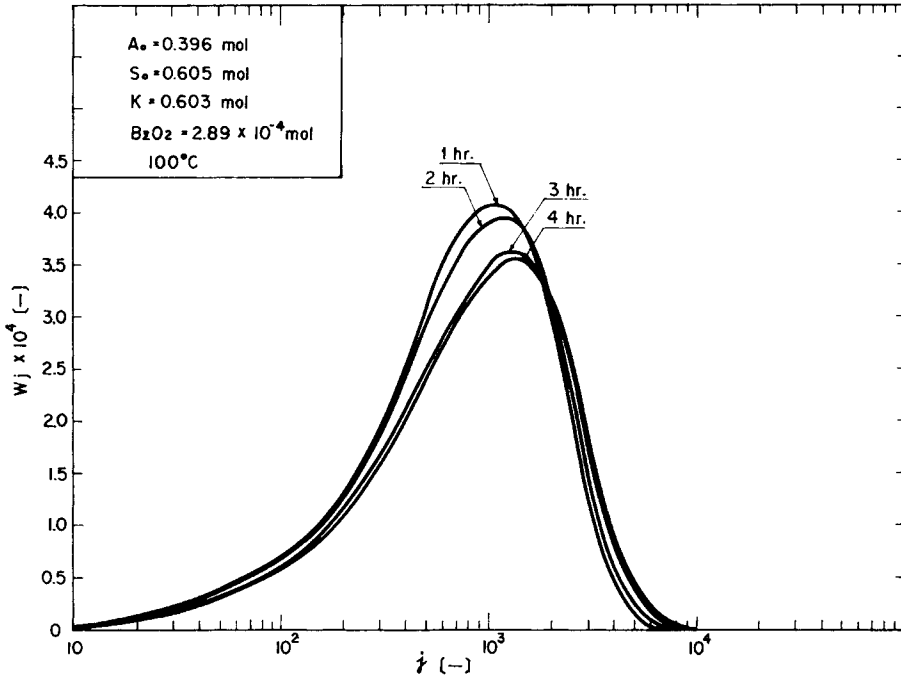


Fig. 7. Molecular weight distribution of copolymer obtained by GPC.

or

$$\bar{P}_n = \frac{[M_0] - [M]}{\int_0^t [(k_{fK}[K] + k_{fM}[M])h(\beta/(1 - \beta)) + \frac{1}{2}k_t h^2(\beta/(1 - \beta)^2 - \beta/(1 - \beta))] dt} \quad (44)$$

The number-average molecular weight can be obtained according the following calculation:

$$\bar{M}_n = \bar{P}_n \left(104 \times \frac{1.53}{2.53} + 53 \times \frac{1}{2.53} \right) \quad (45)$$

For weight chain length, it yields

$$\bar{P}_w = \frac{\sum_{j=1}^{\infty} j^2 [P_j]}{\sum_{j=1}^{\infty} j [P_j]} = \frac{\int_0^t [(k_{fK}[K] + k_{fM}[M])h(\beta(1 + \beta)/(1 - \beta)^3) + \frac{1}{2}k_t h^2(\beta(1 + 4\beta + \beta^2)/(1 - \beta)^4 - \beta(1 + \beta)/(1 - \beta)^3)] dt}{[M_0] - [M]} \quad (46)$$

The weight-average molecular weight is thus

$$\bar{M}_w = \bar{P}_w \left(104 \times \frac{1.53}{2.53} + 53 \times \frac{1}{2.53} \right) \quad (47)$$

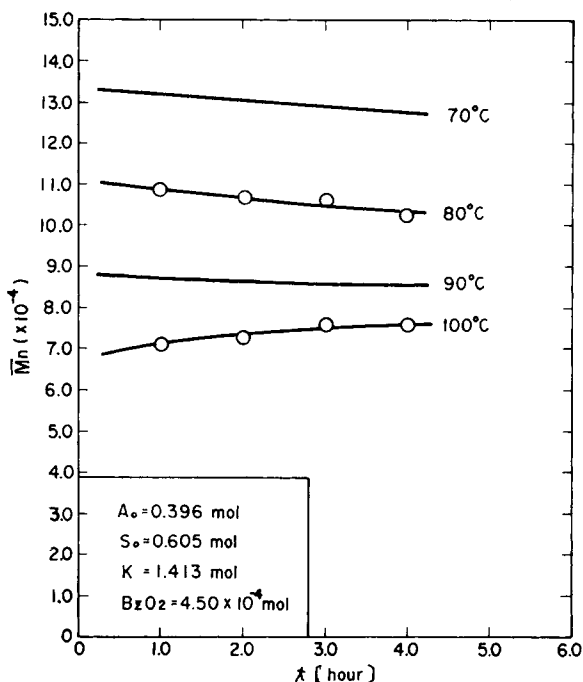


Fig. 8. Effect of reaction temperature on average molecular weight as function of time. (Two sets of experimental data are represented by points.)

Computer programs have been developed to calculate the copolymerization rate, conversion, molecular weight, and molecular weight distribution (MWD) for acrylonitrile–styrene copolymerization. The values of rate constants used are mostly taken from a polymer handbook.⁸ For a few chain transfer constants which could not be found in the literature, reasonable values have been assumed for the present calculation. Principally, however, all the rate constants can be obtained by computer simulation by using this model of reaction kinetics.

EXPERIMENTAL

Polymerization was carried out in a sealed tube by using the ordinary experimental technique, and polymer formed was recovered by evaporation of the solvent at high temperature and under vacuum to determine the conversion. Benzoyl peroxide (BzO_2) as initiator and toluene as solvent were used in this investigation. Solid product obtained was used for the measurements of molecular weight and MWD by GPC (Waters Associates ALC/GPC 200).*

Nitrogen content of the polymer products was determined by an HCN coder (Yanaco MT-2). Applying the simulation model proposed above, a program was written to calculate the rate of reaction, the conversion, and MWD. The computer used was a CDC 3150, which has sufficient storage for our purposes.

* The pore sizes of four consecutive columns were 500, 10^3 , 10^4 , and 10^5 Å. The flow rate of solvent of THF was 1 ml/min, at 25°C. The elution volume can be related to molecular weight by means of a "universal calibration curve." The method proposed by Smith¹² was used to correct for the GPC instrument spreading.

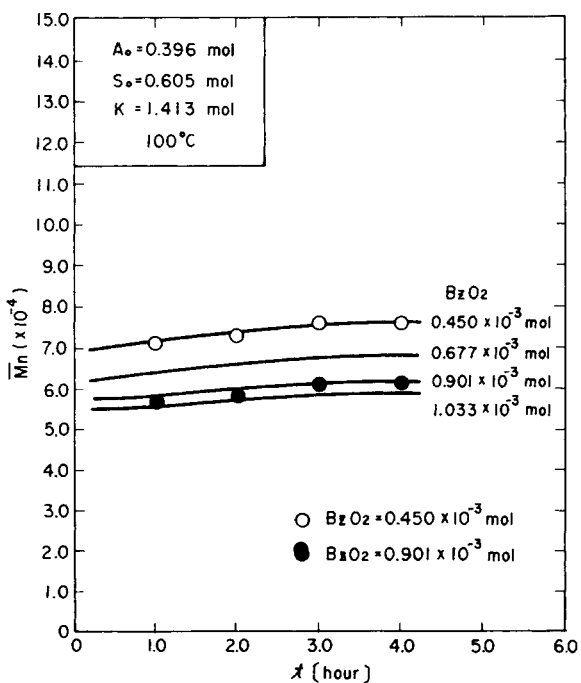
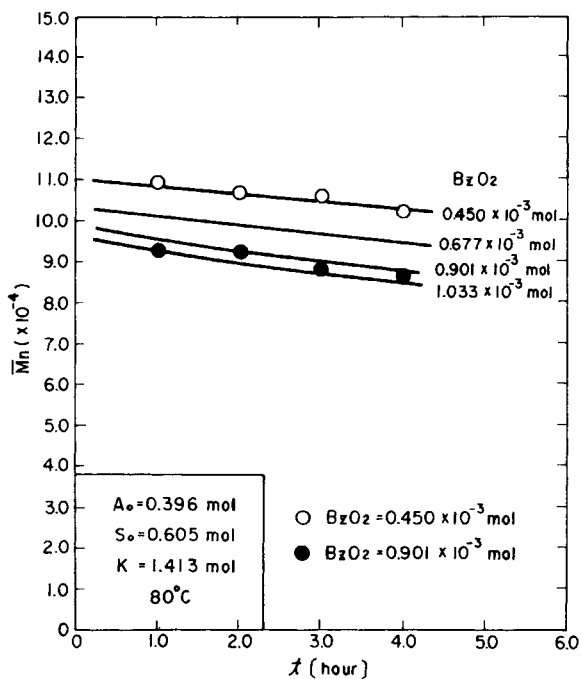


Fig. 9. Effect of initiator concentration on average molecular weight as function of time under reaction temperature of 80°C (a) and 100°C (b). (Two sets of experimental data are represented by points.)

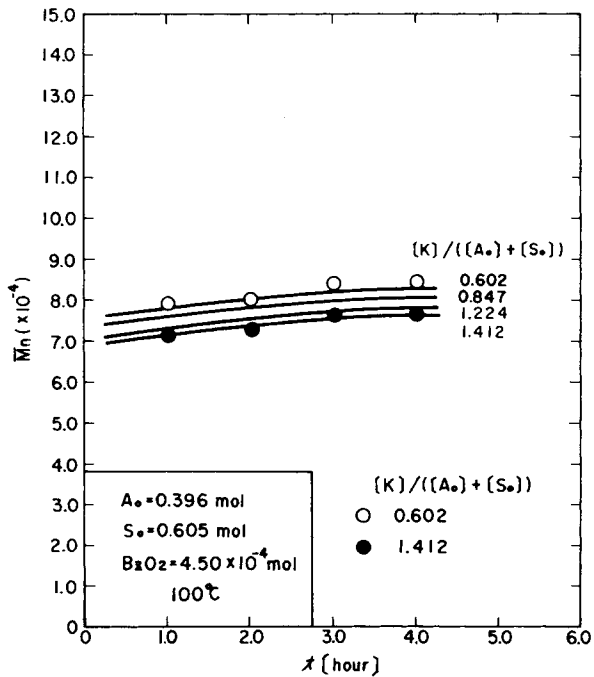
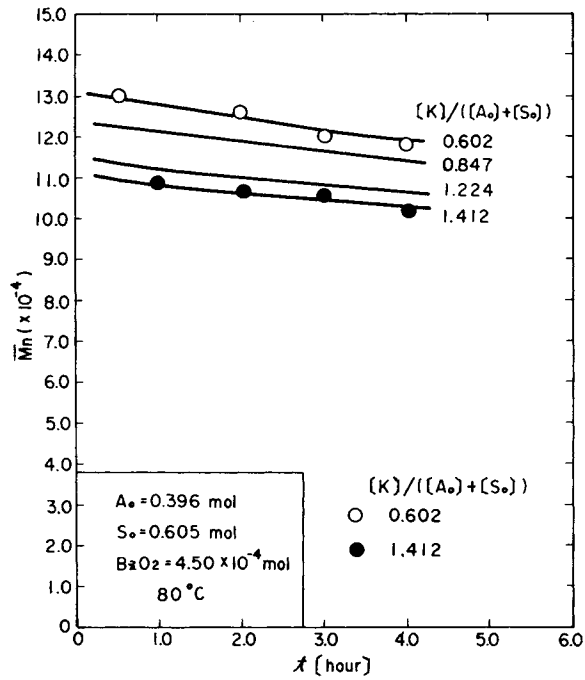


Fig. 10. Effect of solvent-monomer ratio on average molecular weight as function of time under reaction temperature of 80°C (a) and 100°C (b). (Two sets of experimental data are represented by points.)

RESULTS AND DISCUSSION

Azeotropic Composition

Normally, acrylonitrile-styrene copolymer is produced with a sufficient balance in monomer composition. An azeotropic mixture of AN:St = 25:75 by weight is therefore introduced in our model. As shown in Table I, two typical examples of copolymer prepared under azeotropic composition had almost the same proportion of mers throughout the reaction course. The assumption of an azeotropic composition of polymer formed throughout the entire reaction course in our simulation model is entirely justifiable.

Initiator Efficiency

Figure 2 shows two typical examples of conversion versus time curves for the solution copolymerization with and without an initiator. The polymerization without initiator is thermally activated. The initiation consists therefore of chemical and pure thermal initiation steps in this solution polymerization. It is also well known that the initiator efficiency becomes a function of monomer concentration for a low efficiency.⁹ It is found, however, that effective initiator efficiency, including chemical and thermal initiations, can be expressed as the following empirical relationship for this system over a reaction range of a limiting conversion until about 50% and it is not necessary to estimate the value of η , a , and b in eq. (2) by simulation:

$$f = 0.0956([A_0] + [S_0]) \quad (48)$$

Above 50% conversion, an autoacceleration was observed, but further study in this region has not been made in this work, because most industrial operation is limited at this level. It is therefore not necessary to include the autoacceleration effect in this model. As a result of the compensation effect, the two different initiation steps lead to an effective initiator efficiency, including chemical and thermal initiations, which is dependent on the initial concentration of monomers only. This means that the effective initiator efficiency is nearly constant over the entire reaction course of a limiting conversion in this system.

TABLE I
Results of Elemental Analysis of Copolymer Samples^a

Reaction temp., °C	Time, hr	C, H, N content, wt-%			A/S by weight calcd
		C	H	N	
100	1	86.5	7.35	6.15	23.3/76.7
100	2	86.3	7.20	6.50	24.6/75.4
100	3	85.8	7.20	7.00	26.5/73.5
100	4	86.6	6.90	6.50	24.6/75.4
80	1	86.3	7.30	6.40	24.3/75.7
80	2	85.9	7.35	6.75	25.5/74.5
80	3	86.6	7.30	6.10	23.1/76.9
80	4	86.2	7.20	6.60	25.0/75.0

^a Reaction mixture: K = 64 ml, S₀ = 70 ml, A₀ = 26 ml, BzO₂ = 0.07 g.

Conversion and Rate of Polymerization

Figures 3, 4, and 5 show the effects of the temperature, initiator concentration, solvent-monomer ratio on the conversion, and the rate of polymerization, respectively. The solid lines were calculated from the simulation model of eqs. (17) and (19) using the values of the constants and parameters listed in Table II. As mentioned, most rate constants used were taken from a polymer handbook.⁸ Some rate constants at the different temperatures are calculated by expressing the rate constants in their Arrhenius form: $k = A \exp(-E/RT)$. Some parameters that were not available were determined by using an identical set of values which agree with the experimental results obtained at various reaction conditions according to the flow chart shown in Figure 1.

The experimental values are represented by points. Taking into account the fact that the initiator efficiency obeys the empirical relationship of eq. (48), it may be seen that the agreement between the model and experiment is fairly good over the limiting range of conversion.

Average Molecular Weight and Molecular Weight Distribution

In this section the theoretical and experimental results for molecular weight average and MWD are compared and discussed. The chain transfer constants were determined by fitting the experimental data by GPC to the calculated values by computer simulation using the eq. (45).

Figure 6 shows a typical example of change in MWD curves over the several reaction times calculated by computer simulation of the model. Figure 7 shows a typical experimental result obtained by GPC. These two features of MWD are almost identical. Figures 8, 9, and 10 are the \bar{M}_n values calculated as a function of reaction time under the various reaction variables. The values of \bar{M}_n obtained from the analysis of the experimental data are also plotted by points in the figures for comparison, with good results. The chain transfer constants

TABLE II
Numerical Values Used for Computer Simulation

Constant of parameter	Values	Units	Reference ^a
f	$0.0956([A_0] + [S_0])$		*
k_{p11}	$2.28 \times 10^{11} \exp(-5.133 \times 10^3/T)$	[l./g-mole-sec]	*
k_d	$3.22 \times 10^{14} \exp(-1.5395 \times 10^4/T)$	[l./sec]	8
k_{t11}	$2.895 \times 10^{25} \exp(-1.188 \times 10^4/T)$	[l./g-mole-sec]	8
k_{p22}	$4.729 \times 10^7 \exp(-3.557 \times 10^3/T)$	[l./g-mole-sec]	*, 6
k_{t22}	$1.255 \times 10^9 \exp(-844/T)$	[l./g-mole-sec]	6
k_{p21}	$k_{p22}/0.386$	[l./g-mole-sec]	8
k_{p12}	$k_{p11}/0.06$	[l./g-mole-sec]	8
k_{t12}	$160(k_{t11} \times k_{t22})^{1/2}$	[l./g-mole-sec]	10
k_{f11}	$1.5 \times 10^{-4} k_{p11}$	[l./g-mole-sec]	8
k_{f22}	$6.93 \times 10^6 \exp(-5.837 \times 10^3/T)$	[l./g-mole-sec]	*
k_{f12}	$30 \times k_{f11}$	[l./g-mole-sec]	*
k_{f21}	$5 \times k_{f22}$	[l./g-mole-sec]	*
k_{f1K}	$2 \times 10^{-3} k_{p11}$	[l./g-mole-sec]	8
k_{f2K}	$1.95 \times 10^{-4} k_{p22}$	[l./g-mole-sec]	8

^a * = Obtained by this computer simulation.

obtained by the simulation were $k_{f12} = 30 \times k_{f11}$ and $k_{f21} = 5 \times k_{f22}$, which give MWD curves most closely related to the experimental curves.

It has often been shown that average molecular weight at 80°C decreases as the reaction time increases, whereas that at 100°C increases as the reaction time increases. On the other hand, the ratio \bar{M}_w/\bar{M}_n at 80°C remains almost constant as the reaction time increases, whereas that at 100°C increases as the reaction time increases. This fact is very important for the commercial preparation of this kind of copolymer (see Fig. 11).

Monomer Reactivity Ratios

Further, the monomer reactivity ratios r_1 and r_2 of copolymerization can be theoretically estimated by using this simulation model. Under the condition of $d[A]/d[S] = [A]/[S]$ in an azeotropic mixture, the copolymerization equation can be obtained by eq. (3)/eq. (4) in our model and is reduced to

$$[A]/[S] + r_2 = r_1 [A]/[S] + 1 \quad (49)$$

where $[A]/[S] = 1/1.53$, and r_1 and r_2 calculated from eq. (49) are $r_1 = 0.06$ and $r_2 = 0.386$, respectively. These values agree quite well with documented material.⁸

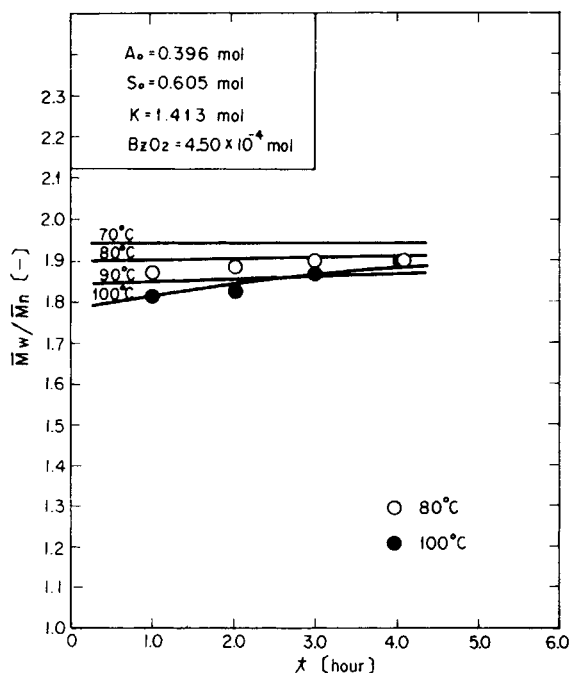


Fig. 11. Effect of reaction temperature on ratio \bar{M}_w/\bar{M}_n as function of time. (Two sets of experimental data are represented by points.)

CONCLUSIONS

A new model for the rate of polymerization of acrylonitrile and styrene in toluene as solvent is proposed. The differential rate equations for copolymerization derived from the model are transformed into differential equations for the homopolymerization under an azeotropic composition. These differential equations have been solved on a digital computer to simulate or predict the conversion and molecular weight distribution as a function of time. Even though the solution copolymerization includes very complex elemental steps with many parameter constants that are usually not available in the literature, experimental results obtained over the usual range of temperature, initiator concentration, and solvent concentration were successfully correlated to limiting conversion by this model. This model provides the design, simulation, and optimization of homogeneous solution copolymerization reactors. The model proposed is therefore suitable for a system of reaction temperature range of 80–100°C, initiator–monomer mole ratio of 3×10^{-4} – 9×10^{-4} , and a solvent–monomer mole ratio of 0.6–1.4 until 50% conversion.

Nomenclature

A	acrylonitrile
A_0	acrylonitrile at initial condition
[A]	concentration of acrylonitrile (g-mole/l)
$[A_0]$	initial concentration of acrylonitrile (g-mole/l)
f	efficiency of initiator
I	initiator
$[I_0]$	initial concentration of initiator (g-mole/l)
[I]	concentration of initiator (g-mole/l)
K	solvent
[K]	concentration of solvent (g-mole/l)
\bar{M}_n	number-average molecular weight (g/g-mole)
\bar{M}_w	weight-average molecular weight (g/g-mole)
P_j	polymer with j monomer units
$[P_j]$	concentration of polymer with j monomer units (g-mole/l)
\bar{P}_n	number average chain length
\bar{P}_w	weight average chain length
r_1	monomer reactivity ratio = k_{p11}/k_{p12}
r_2	monomer reactivity ratio = k_{p22}/k_{p21}
R^*	a radical
R_j^*	growing radical with j units
R_i	rate of initiation (g-mole/l-hr)
$[R_j^*]$	concentration of growing radical with j units (g-mole/l)
R_p	rate of polymerization (g-mole/l-hr)
R_t	rate of termination (g-mole/l-hr)
R_T	= $\Sigma [R_j^*]$ (g-mole/l)
S	styrene
S_0	styrene at initial condition
[S]	concentration of styrene (g-mole/l)
t	reaction time (hr)

T	temperature (K)
X	conversion
X_T	total radical concentration of acrylonitrile ending (g-mole/l)
X_j^*	growing radical with acrylonitrile ending and j monomer units
Y_T	total radical concentration of styrene ending (g-mole/l)
Y_j^*	growing radical with styrene ending and j monomer units
η, a, b	constants
W_j	weight fraction of polymer P_j in total polymer

References

1. K. Arai and S. Saito, *J. Chem. Eng. (Japan)*, **9**, 302 (1976).
2. J. C. Hyun, W. W. Graessley, and S. G. Bankoff, *Chem. Eng. Sci.*, **31**, 945 (1976).
3. W. H. Ray, *J. Macromol. Sci.-Rev. Macromol. Chem.*, **C8**(1), 1 (1972).
4. L. T. Fan and J. S. Shastry, *J. Polym. Sci. Macromol. Rev.*, **7**, 155 (1973).
5. J. H. Duerksen, A. E. Hamielec, and J. W. Hodgins; *A.I.Ch.E.J.*, **13**, 1081 (1967).
6. A. E. Hamielec, J. W. Hodgins and K. Tebbens, *A.I.Ch.E.J.*, **13**, 1087 (1967).
7. C. C. Lin and W. Y. Chiu, *Bull. Coll. Eng. (National Taiwan University)*, **21**, 221 (1977).
8. J. Brandrup and E. H. Immergut, Eds., *Polymer Handbook*, 2nd ed., Wiley, New York, 1975.
9. P. J. Flory, *Principles of Polymer Chemistry*, George Banta, Menasha, Wisconsin, 1967, p. 113.
10. M. Suzuki, H. Miyama, and S. Fujimoto, *Bull. Chem. Soc. (Japan)*, **35**, 60 (1962).
11. E. A. Collins, J. Bares, and F. W. Billmeyer, Jr. *Experiments in Polymer Science*, Wiley, New York, 1973 p. 161.
12. W. V. Smith, *J. Appl. Polym. Sci.*, **18**, 925 (1974).

Received August 23, 1977

Revised February 10, 1978